Science of the Total Environment 947 (2024) 174681

Contents lists available at ScienceDirect

Science of the Total Environment

journal homepage: www.elsevier.com/locate/scitotenv

Multi-decadal geochemical evolution of drainage from underground coal mines in the Appalachian basin, USA

C.R. Schaffer [a,*], C.A. Cravotta III [b], R.C. Capo [a], B.C. Hedin [c], D.J. Vesper [d], B.W. Stewart [a]

[a] Department of Geology and Environmental Science, University of Pittsburgh, Pittsburgh, PA, USA
[b] Cravotta Geochemical Consulting LLC, Bethel, PA, USA
[c] Hedin Environmental, Inc., Pittsburgh, PA, USA
[d] Department of Geology and Geography, West Virginia University, Morgantown, WV, USA

HIGHLIGHTS

- Evaluation of spatiotemporal factors of Appalachian coal mine drainage chemistry
- Contaminant decay rates and initial concentrations increase with minepool depth.
- A geochemical evolution model explains temporal and spatial contaminant trends.
- Siderite equilibrium likely controls long-term steady-state Fe concentrations.
- Cation-exchange processes result in evolution to Na-HCO_3-SO_4 water-type.

GRAPHICAL ABSTRACT

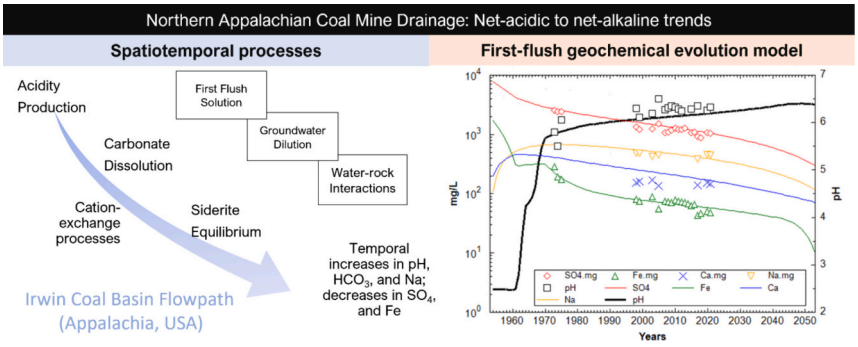

ARTICLE INFO

Editor: JV Cruz

Keywords:
Acid mine drainage
Geochemistry
Cation exchange/ion exchange
Siderite
First-flush
Contaminant prediction

ABSTRACT

Coal mine drainage (CMD) in Appalachia is a widespread source of dissolved metals, SO_4, and acidity that can degrade aquatic habitats and water supplies for decades following mine closure and flooding. In the bituminous coalfield of Pennsylvania, the Irwin Coal Basin (ICB) contains a series of partly to completely flooded, abandoned underground mines separated by leaky barriers within the Pittsburgh coal seam. CMD originated throughout the basin from minepool aquifers that formed after mine closures dating from 1910 to 1957. Historical and recent water quality data for eight CMD sites across the ICB, plus mineralogy and cation-exchange capacity of overburden lithologies, were analyzed to quantify important reactants and evaluate spatial and temporal water-quality trends. As overburden thickness and residence time increase along a ~ 50-km flowpath northeast to southwest in the basin, CMD becomes more alkaline, and Na concentrations increase. Since the 1970s, all eight ICB discharges have become less acidic, with exponential decreases in acidity, SO_4, and Fe concentrations; only two CMD remain net-acidic (acidic pH at equilibrium). Exponential decay models that include a steady-state asymptote consistent with background groundwater chemistry and siderite equilibrium describe the early-stage, rapid contaminant concentration decay immediately after the "first flush" (initial flooding) and the progressive evolution toward late-stage background conditions. A geochemical evolution PHREEQC model indicates that spatial and temporal trends in pH, net-acidity, SO_4, Fe, and major cations could be explained by the

* Corresponding author.
E-mail address: CAS420@pitt.edu (C.R. Schaffer).

https://doi.org/10.1016/j.scitotenv.2024.174681
Received 27 December 2023; Received in revised form 7 July 2024; Accepted 8 July 2024
Available online 10 July 2024

continuous dilution of first flush water by ambient groundwater combined with sustained water-mineral reactions involving pyrite and carbonates (calcite, dolomite, siderite) plus cation-exchange by clays (illite, chlorite, mixed-layer illite/smectite). These data and model results indicate that 1) cation-exchange reactions enhance calcite dissolution and alkalinity production, resulting in the evolution of CMD to Na-SO_4-HCO_3 type waters, and 2) siderite equilibrium could maintain dissolved Fe >16 mg/L over the next 40 years.

1. Introduction

Contaminant loading from coal and metal mines degrades water supplies and aquatic ecosystems and diminishes the potential for economic development and recreational activities in historically mined areas around the world (Zeman et al., 2009; Nordstrom, 2011a, 2011b; Huisamen and Wolkersdorfer, 2016; Acharya and Kharel, 2020; Wang et al., 2023). In the Northern Appalachian Coalfield of northeastern USA, legacy coal mine drainage (CMD) can have pH as low as 2.7, with dissolved iron (Fe), aluminum (Al), manganese (Mn), and sulfate (SO_4) concentrations >500 mg/L, 100 mg/L, 70 mg/L, and 2000 mg/L, respectively (Cravotta III, 2008a; Cravotta III and Brady, 2015; Vass et al., 2019). The release of acidity, SO_4, Fe, Al, Mn, and other metals by CMD generally continues for decades after mine closure due to the gradual dilution of initially acidic "first flush" minewater and the continued interaction of oxygen with pyrite in the overburden and unmined coal (Cravotta III, 1994, Younger, 2000; Zeman et al., 2009; Eriksson and Daniels, 2021).

Long-term studies of CMD chemistry in the Northern Appalachian Coafield indicate that after mine closure and initial flooding, the contaminant concentrations tend to decrease while the pH and alkalinity increase (Wood, 1996; Capo et al., 2001; Lambert et al., 2004; Demchak et al., 2004; Raymond and Oh, 2009; Burrows et al., 2015). In many cases, CMD may evolve from net-acidic to net-alkaline character, in which the pH at equilibrium with the atmosphere is acidic or circumneutral, respectively (e.g., Rose and Cravotta III, 1998; Kirby and Cravotta III, 2005a, 2005b). Net-acidic CMD may require treatment with neutralizing agents to increase pH and facilitate the removal of Fe, Al, and Mn, whereas net-alkaline CMD may only require treatment for Fe and Mn (e.g., Cravotta III et al., 2015; Skousen et al., 2019; Nordstrom, 2020).

The geochemical behavior of CMD on a decadal time scale is influenced by the local hydrology and time-dependent, non-linear chemical interactions between water, rock, and the atmosphere (Rose and Cravotta III, 1998; Perry, 2001; Nordstrom, 2011a, 2011b; Cravotta III et al., 2014). CMD generated from "above-drainage" mines, which are partially or entirely above the local groundwater hydraulic head (water table), is frequently oxic, with short residence times (< 3 years), which perpetuates pyrite oxidation and acidity production (e.g., Rose and Cravotta III, 1998; Winters and Capo, 2004; McDonough et al., 2005b; Burrows et al., 2015). In contrast, CMD generated from "below-drainage" mines, which are largely below the water table, usually has diminished oxygen supply and longer residence times, which can limit pyrite oxidation while increasing contact time with carbonate minerals, commonly resulting in net-alkaline, circumneutral CMD (Mentz and Warg, 1975; Rose and Cravotta III, 1998; Winters and Capo, 2004; McDonough et al., 2005a; Burrows et al., 2015).

Models that relate hydrology, geology, and the time elapsed since mine closure can help to explain post-mining groundwater quality and long-term CMD contaminant trends (Wood et al., 1999; Younger, 2000; Lambert et al., 2004; Burrows et al., 2015). For example, the first flush phenomenon has been used to describe the initial contaminant peak, exponential decrease, and eventual steady-state behavior of major contaminants in CMD across the Appalachian Coalfield (Mack and Skousen, 2008; Perry and Rauch, 2012, 2013), as well as globally (Younger, 2000; Gyzl and Banks, 2007; Wolkersdorfer, 2008; Zeman et al., 2009; Huisamen and Wolkersdorfer, 2016; Merritt and Power, 2022; Wang et al., 2023). During mining operations, pyrite oxidation products, including relatively soluble SO_4 salts (e.g., copiapite, coquimbite, römerite, and pickeringite), tend to accumulate in the humid, air-filled mine voids (Cravotta III, 1991, 1994; Alpers et al., 1994; Alpers and Nordstrom, 1999; Majzlan et al., 2004, 2006). Following mine closure, groundwater saturates these voids and rapidly dissolves the SO_4 salts, creating an acidic leachate, characterized by elevated concentrations of SO_4, Fe, Al, and other metals (Cravotta III, 1994; Perry, 2001). After this first flush, contaminant concentrations tend to decrease rapidly as continuously introduced groundwater progressively dilutes and neutralizes the leachate (Younger, 2000; Demchak et al., 2004; Perry et al., 2005; Zeman et al., 2009). Eventually, contaminant concentrations in the abandoned mine and associated CMD tend to stabilize and may approach unmined, background groundwater composition or some other steady-state condition. For example, under near-neutral conditions, siderite equilibrium may control Fe^{2+} concentrations in CMD (e.g., Cravotta III, 2008b; Blowes et al., 2014).

Exponential decay models have been widely used to quantify decreases in SO_4, Fe, and acidity of CMD following the first flush (e.g., Mack and Skousen, 2008; Wolkersdorfer, 2008; Perry and Rauch, 2012, 2013; Huisamen and Wolkersdorfer, 2016). Although the late-stage contaminant concentration is critical for determining future remediation obligations or projecting to a future time when concentrations fall below the maximum contaminant level (MCL), most CMD decay models assume contaminant concentrations eventually reach zero, which is unrealistic. A few studies have incorporated a non-zero asymptote value to account for the long-term approach to background groundwater composition or other specified steady-state conditions (e.g., Gyzl and Banks, 2007; Merritt and Power, 2022). Nevertheless, hydrogeochemical processes affecting the selected asymptote values and timing for CMD systems that evolve from net-acidic to net-alkaline conditions have not been previously considered.

Thus, understanding the factors affecting relations among pH, alkalinity, and dissolved metals in CMD and how these characteristics vary over time is needed to develop predictive models of long-term changes in water quality and contaminant loading. This predictive modeling applies to developing adaptive strategies for cost-effective remediation of CMD, managing long-term post-mining obligations, and mitigating potential effects of CMD on surface water chemistry.

This paper considers new approaches for development of exponential decay models plus a hydrogeochemical model of the first-flush phenomenon that are broadly applicable for describing widely observed long-term trends for SO_4, metals, major ions, and pH of CMD. The spatial and temporal evolution of CMD from a series of sites in a historically mined basin in the Northern Appalachian Coalfield is presented as a case study. The Irwin Coal Basin (ICB) contains CMD that varies from net-acidic to net-alkaline character (Fig. 1b). From northeast to southwest, increasing overburden thickness (30 to 94 m), residence time (1 to 11 years), and minepool flooding (22–100 %) have resulted in a CMD geochemical gradient spanning a wide range of Appalachian CMD chemistry (Fig. 1a–c) with increasing pH (~3–7) and alkalinity (0–300 mg/L as $CaCO_3$) (Weaver et al., 1998; Capo et al., 2001; Winters and Capo, 2004). For this case study, we integrate basin hydrogeology, overburden mineralogy, and temporal and spatial CMD chemistry into hydrogeochemical evolution models that indicate past and future CMD water-quality trends. The study serves to 1) identify important water-rock reactions and hydrological factors that affect spatiotemporal evolution patterns of CMD, 2) quantify the long-term decrease of major CMD contaminant concentrations using first- and second-order decay

models with asymptote values constrained by geochemical processes, and 3) simulate the net-acidic to net-alkaline evolution of CMD using a generalized forward geochemical modeling approach.

2. Study area

The Appalachian Coalfield extends as a long, narrow band across seven states in the eastern United States (>1300 km long, <200 m wide) (Fig. 1a), and the ICB is situated in the bituminous coalfields of the northeastern section (Winters and Capo, 2004). The ICB is a typical large (240 km^2) coal basin within a series of anticlines and synclines west of the Allegheny orogenic front in the Appalachian Mountains in southwest Pennsylvania (Fig. 1a). An important geologic feature, the Pittsburgh coal seam, is approximately 2 m thick and forms the basal unit of the Pennsylvanian Monongahela Group, which contains alternating cyclothem sequences of sandstone, shale, and limestone (Fig. S1a) (Brady et al., 1998; Edmunds, 1999; Winters and Capo, 2004).

Extensive extraction of Pittsburgh coal by room-and-pillar methods occurred from the 1850s to 1984. Flooding after mine closure resulted in post-mining aquifers or "minepools" made up of mine voids plus partially collapsed overburden. Winters and Capo (2004) delineated eight minepool subbasins across the ICB, whereby unmined coal barriers restricted flow between subbasins and the associated CMD outfall maintained the hydraulic head within a subbasin (Fig. S1b). The two northern subbasins, Delmont and Export, are above-drainage mines and are isolated from mines to the south by an intact coal barrier (under a railroad line cutting across the basin), with water elevation strongly influenced by recharge along subsidence-induced fractures (Winters and Capo, 2004). Deeper, below-drainage minepools to the south are likely in communication with one another due to leakage through remnant mine barriers and slight differences in the hydraulic head, and recharge is influenced by overlying aquifers (Winters and Capo, 2004).

This study investigates CMD originating from eight minepool subbasins across the ICB: Export, Delmont, Coal Run, Irwin, Upper Guffey, Lower Guffey, Lowber, and Douglas Run (Fig. 1a). The minepools formed after mines closed between 1910 and 1957, and CMD sampling data are available since the 1970s. Alkalinity (as $CaCO_3$) of ICB discharges ranges from 0 to 0.5 mmol/L or 0–25 mg/L, 2.4 to 4.0 mmol/L or 120–200 mg/L, and 5.0 to 8.0 mmol/L or 250–400 mg/L and are denoted by the red, yellow, and blue symbols, respectively, in Fig. 1.

3. Methodology

3.1. Core sampling and analysis

Rock samples were analyzed to determine mineral composition and chemical properties, which are needed to explain possible groundwater-rock interactions in post-mining aquifers. Unweathered rock, representative of the Monongahela Group in the ICB, was subsampled from a 90-m core drilled by the Pennsylvania Geological Survey to approximately 1 m below the Pittsburgh coal seam in Fayette County, Pennsylvania (FAY051022), the nearest available core location ~20 km southeast of the ICB (Fig. 1a). The sampling interval was chosen to represent lithologies likely to interact with CMD in the post-mining coal seam aquifer. The post-mining aquifer thickness was assumed to be 17.5 m, assuming the maximum fracture zone height is 7 times greater than the mined coal seam thickness (~2.5 m in FAY051022) (Winters and Capo, 2004). Sixteen subsamples were collected from the interval immediately below the base of the Pittsburgh coal seam to 19 m above to represent coal and associated underclay, and overlying organic-rich shales, calcareous mudstone, siltstone, and sandstone lithologies. Samples were powdered in a tungsten-carbide ball mill and split for analysis. Because

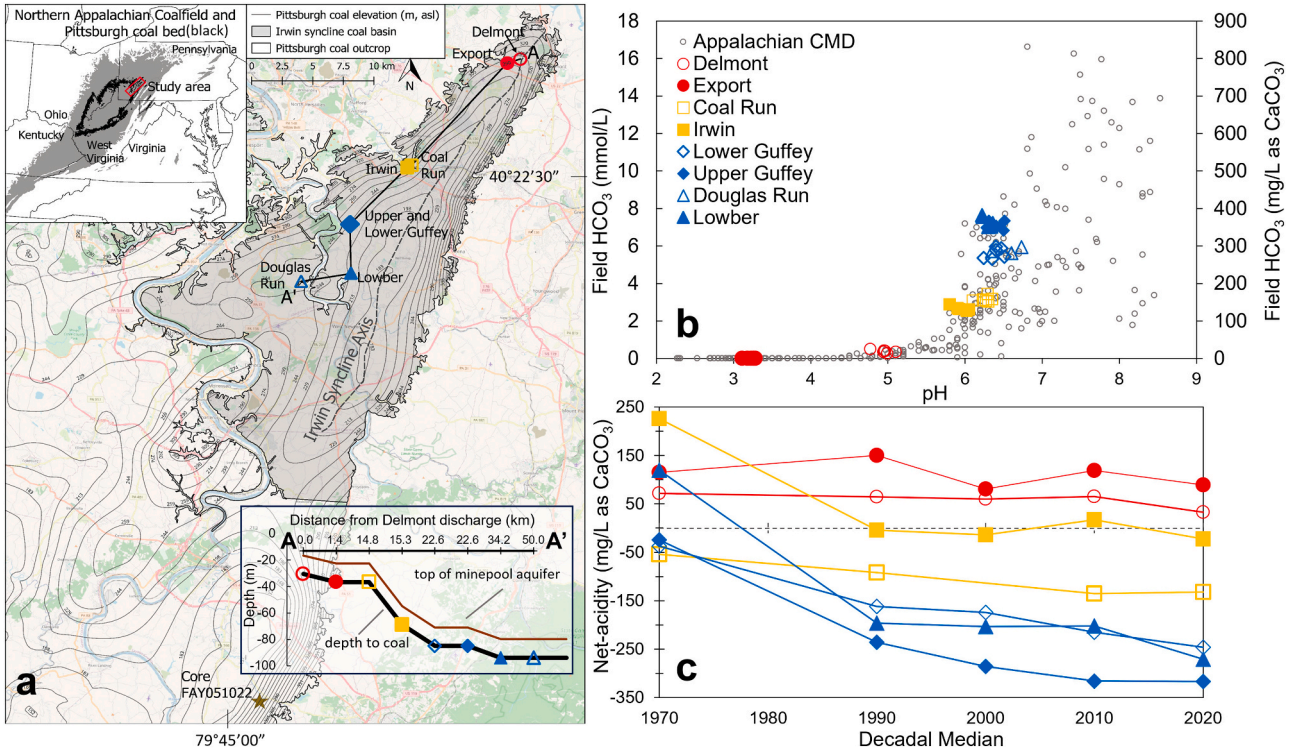

Fig. 1. (a) Map of Irwin Coal Basin (gray) showing elevation of Pittsburgh Coal (m above sea level), and the location of eight CMD discharges (red, yellow, blue symbols) and Core FAY51022 (star symbol). The upper inset shows the location of ICB and the outcrop of the Pittsburgh coal (black) in the northern Appalachian Coalfield. Lower inset shows that the discharges along transect A–A′ originate from minepool aquifers with increasing depth to the Pittsburgh coal seam (Northern and Central Appalachian Basin Coal Regions Assessment Team, 2001; Ruppert et al., 1997). (b) Field alkalinity vs. pH of Northern Appalachian Coalfield (CMD) (n = 286; data from Capo et al., 2001; Cravotta III, 2008a; Cravotta III and Brady, 2015; and J. Hawkins, personal communication) and the Irwin Coal Basin (ICB) (large symbols; this study). (c) The deeper sites evolved from net-acidic to net-alkaline character over decadal timeframe (no historical data are available for Douglas Run).

of the small sample sizes, the splits were combined to represent the major overburden lithologies.

XRD analysis of each major overburden lithology was carried out by K/T GeoServices, Inc. This included bulk materials and clay (<4 μm fraction) using a Siemens D500 automated powder diffractometer equipped with a copper X-ray source (40 kV, 30 mA) and a scintillation X-ray detector. Clay identification was carried out both on air-dried and ethylene glycol-solvated oriented clay mounts. Mixed clay ordering and expandability was determined using the NEWMOD program (Yuan and Bish, 2010).

The cation-exchange capacity (CEC) for each composite lithology sample from the core and four clay standards (kaolinite, montmorillonite, illite and bentonite) was determined at West Virginia University following the unbuffered salt-extraction method of Sumner and Miller (1996). Concentrations of extracted ions (Al^{3+}, Ca^{2+}, K^{+}, Mg^{2+}, and Na^{+}) were measured by ICP-OES at West Virginia University.

3.2. CMD water quality measurements

3.2.1. CMD water sampling and field methods

Eight CMD sites in the ICB (Fig. 1) were sampled every other month from October 2020 to August 2021 to document spatial variations in CMD composition. Flow rate was measured using a handheld flowmeter across a transect at larger discharges and by timing the fill of a 19 L bucket at smaller sites. The pH, dissolved oxygen, specific conductance, and oxidation-reduction potential (ORP) were measured in-situ using a YSI multi-probe. The pH electrode was calibrated in pH 4 and 7 buffers, ORP in ZoBell's solution, and dissolved oxygen was calibrated to 0 % and 100 % saturation before each sampling event. Measured ORP values were converted to Eh using ZoBell's temperature correction (Nordstrom, 1977). Field alkalinity was determined using a Hach digital titrator, 1.6 N H_2SO_4 alkalinity test kits, and gran titration at pH 4.2 and 3.9 end points. The units of alkalinity are expressed as mg/L as $CaCO_3$ (American Public Health Association, 2000; Thomas and Lynch, 1960). The CO_2 and dissolved inorganic carbon (DIC) samples were collected underwater (in situ or in a bucket), with zero headspace using pre-washed bottles (~500 mL) rinsed in triplicate with the sample water before collection, capped tightly, and sealed with electrical tape. Samples for cation analysis were filtered on-site through 0.45 μm nylon filters and acidified in the field to 2 % HNO_3, while filtered, unacidified samples for anion analysis were stored on ice and then refrigerated until analyzed.

3.2.2. CMD water sample analysis

Major and trace metals of CMD water samples were analyzed by inductively coupled plasma mass spectrometer (ICP-MS) at a third-party laboratory (Activation Laboratories, Ltd.). Anions were measured at West Virginia University using ion chromatography (IC). Dissolved CO_2 was measured on an Anton Paar CarboQC Carbonation Meter following a method modified from Vesper and Edenborn (2012) to allow transport from field to laboratory for analysis; samples were introduced to the CarboQC under a pressurized N_2 blanket via the Anton Paar Pressurized Filling Device. For use as input for speciation modeling, CO_2 concentrations measured in the laboratory were converted to DIC concentrations at field temperature using temperature-corrected equilibrium constants from Plummer and Busenberg (1982). First, the measured dissolved CO_2 concentration was converted back to partial pressure of CO_2 (P_{CO2}) using the Henry's Law constant (K_{CO2}) at the temperature of laboratory measurement. Second, the P_{CO2} calculated in the first step was converted into a dissolved CO_2 concentration using the K_{CO2} at the field temperature. The dissolved CO_2 concentration was used with the field-measured pH to compute the major carbonate species activities and, considering activity coefficients, the corresponding concentration of DIC (= $[CO_2] + [H_2CO_3] + [HCO_3^-] + [CO_3^{2-}]$, where brackets indicate molar concentrations).

3.2.3. Historical CMD water data

Historical data on chemistry of CMD water in the ICB were compiled from several sources, providing a decades-long record of selected chemical parameters. Although data were not available for the initial period immediately after mine flooding, the studied CMD sites were sampled systematically in the 1970s and reported in the so-called "Scarlift Reports" (Pullman Swindell Inc., 1977). Additionally, the same CMD sites were sampled at various times from 1998 to 2020 and results reported by Weaver et al. (1998), Capo et al. (2001), Pennsylvania Department of Environmental Protection (variously dated unpublished reports), Hedin Environmental (2013), and Cravotta III (2008a). The Supplemental information (Table S3) summarizes all the historical data. In addition, Northern Appalachian regional deep CMD data ($n = 286$) were compiled from Cravotta III (2008a, 2008b), Cravotta III and Brady (2015), and J. Hawkins (personal communication) and included in Figs. 1b and S2.

3.3. First and second-order decay rate equations

In this work, both first- and second-order equations are considered to explain the observed shifts in CMD chemistry over time, with a steady-state constant to account for late-stage asymptote values (Langmuir, 1997; Cravotta III, 2008c):

$$\frac{dC}{dt} = -k \bullet (C - C_s)^n \tag{1}$$

where t is time (yr), C is concentration (mg/L), C_S is steady-state concentration (mg/L), k is the rate constant (yr^{-1}), and n is the order of the reaction. For a first-order decay model, where n is 1, integrating Eq. (1) and rearranging terms results in:

$$C(t) = (C_0 - C_s) \bullet e^{-k't} + C_s \tag{2}$$

where k' is the first-order rate constant, and C_0 is the initial concentration. For a second-order decay model, where n is 2, integration and rearranging terms results in:

$$C(t) = C_s + \frac{1}{-k''t + \frac{1}{(C_0 - C_s)}} \tag{3}$$

where k'' is the second-order rate constant. A key difference between Eqs. (2) and (3) is that the second-order model is dominated by the C_0-C_S term resulting in a sharper initial decay.

To calculate initial time, it was assumed that CMD flooded the subbasin before discharge; residence time reported by Winters and Capo (2004) was added to the year of mine closure of each ICB subbasin, except for Irwin which flooded between 1955 and 1957 according to Pullman Swindell Inc. (1977). Annual medians of Fe, SO_4, and net-acidity data were used to de-emphasize years with frequent sampling. Both decay equations were fit with data from seven CMD sites within the ICB, and C_0 and k' or k'' were quantified using nonlinear least squares regression (MathWorks Inc., 2023).

3.4. Geochemical models

3.4.1. Aqueous speciation

Aqueous speciation and saturation indices of major minerals for the 2020–2021 water samples were calculated using PHREEQC version 3.7.3 (Parkhurst and Appelo, 2013) with the wateq4f thermodynamic database (Ball and Nordstrom, 1991), which is widely used to evaluate speciation of trace metals in acid mine drainage (Alpers and Nordstrom, 1999; Cravotta III, 2008b; Nordstrom and Campbell, 2014; Nordstrom, 2020). Measured ORP values were converted to Eh using the Zobell's temperature correction and the water temperature measured in the field (Nordstrom, 1977). The pe, computed from Eh using the Nernst equation with sample temperature, was used to set the redox conditions to

estimate Fe^{II} and Fe^{III} fractions.

We compared the (1) field alkalinity to computed alkalinity based on DIC input, and (2) the CarboQC measured values for the Pco_2 and DIC to those computed from input alkalinity (Fig. S3). Typically, measured field alkalinity is the input component for inorganic carbon in PHREEQC models (e.g., Perry, 2001); in some cases, DIC or P_{CO2} are specified to represent environmental conditions (e.g., Burrows et al., 2015). However, unlike CO_2 and corresponding DIC, field alkalinity cannot be measured at low pH values (<4.2 using Gran titration). Only one input component for inorganic C can be considered for a set of speciation computations by PHREEQC, either the concentration of alkalinity or DIC (input as C(4)) (e.g., Pötter et al., 2021). Because comparison indicated comparable results (Fig. S3), temperature corrected DIC concentration data from the CarboQC were used in PHREEQC speciation and reaction models, which span pH values from 3 to 7.

The CMD net acidity, in mg/L as $CaCO_3$, was computed from the field-measured pH, the field-measured alkalinity, in mg/L as $CaCO_3$, and the total dissolved concentrations (C) of Fe^{II}, Fe^{III}, Mn, and Al, in mg/L, using the following expression (Kirby and Cravotta III, 2005a, 2005b):

$$\text{Net} - \text{acidity} = 50\left[1000\left(10^{-ph}\right) + \frac{2(C_{Fe^{II}})}{56} + \frac{3(C_{Fe^{III}})}{56} + \frac{2(C_{Mn})}{55} + \frac{3(C_{Al})}{27}\right] - \textit{Alkalinity} \quad (4)$$

Net-alkaline samples have a negative value for net acidity, which indicates sufficient buffering to maintain circumneutral pH (> 6.0) after outgassing of CO_2 and hydrolysis of Fe, Mn, and Al under equilibrium conditions with the atmosphere (Kirby and Cravotta III, 2005a, 2005b). In contrast, net-acidic samples have a positive net acidity and, after equilibration with the atmosphere, will have acidic pH values (< 4.5). In practice, net acidity is important for selection of CMD treatment strategies (e.g. Skousen, 2017).

3.4.2. Forward reaction model

For this study, a novel forward reaction model (detailed in Section 2.0 of Supplemental information) was developed using PHREEQC to quantify the hydrogeochemical processes involved in both the initial development and long-term evolution of minepool water quality over decadal time scales. The forward model simulates (1) initial formation of acidic first flush water by dissolution of pyrite oxidation products; (2) the long-term influx and mixing of ambient groundwater with the progressively evolving minepool water; and (3) potential water-mineral interactions to account for observed changes in chemistry of the associated CMD. The model was applied to simulate the long-term changes in chemistry of the Lowber CMD, a below-drainage mine (Fig. 1), which is representative of evolved, highly mineralized deep minepool water that had undergone net-acidic to net-alkaline transition, including effects from cation exchange. Different model scenarios were considered to evaluate the effects of dilution, mineral dissolution-precipitation reactions, and cation-exchange processes.

The initial first-flush solution (having extremely high total dissolved solids, SO_4, Fe, and low pH) was simulated as a single reaction where ambient groundwater (sample WE-315, McAuley and Kozar, 2006) dissolved coquimbite ($Fe_{1.47}Al_{0.53}(SO_4)_3$: $9.65H_2O$ in model, per Majzlan et al., 2006), a soluble secondary SO_4 salt that represents accumulated pyrite oxidation products formed in humid air prior to mine flooding (e.g. Cravotta III, 1991, 1994), plus carbonate, aluminosilicate, and oxide minerals identified in the core samples (Tables S11–S13). Mn-bearing siderite was considered as a source of Mn (Morrison et al., 1990; Chapman et al., 2013). To simulate attenuation of constituents in any step, equilibrium phases such jarosite, schwertmannite, $Fe(OH)_3$, and siderite were specified to precipitate upon reaching the saturation index indicated in Table S12.

Sequential changes were simulated as a 100-step progression whereby the evolving minepool water was mixed with a constant fraction of ambient groundwater. Time zero represented the first year the Lowber minepool was flooded (1953), and each 'step' represented 1 year. Given the 11.4-year minepool residence time reported by Winters and Capo (2004) assuming a steady-state flow, the groundwater volume fraction added and a corresponding fraction of minepool water discharged each year was calculated as 8.8 % (1 year/11.4 years); by 2021 (year 68), the total groundwater influx equated to six minepool volumes. The same mineral assemblage, including the exchanger having CEC and cation proportions comparable to the measurements of FAY051022 core samples, was reacted in each step, but in quantities progressively decreasing by 1 % per year.

The model was calibrated by adjusting the total quantities of initial mineral reactants until simulation results were comparable to the available historical sample dataset from 1970 to 2021 (Table S3). The forward model was run to 100 years after the initial flush to indicate both the past evolution and potential future composition of CMD. Eh-pH diagrams and Piper plots showing observed data for the 2020–2021 study with the results of the PHREEQC forward model were constructed using Geochemist's Workbench (GWB) Edition 17.0 (Bethke et al., 2021) and the wateq4f database (Ball and Nordstrom, 1991) in GWB format.

4. Results and discussion

Detailed summaries of water chemistry (Tables S1–S5), rock composition (Tables S6–S7), and modeling (Tables S8–S13) data are included in tables and text provided with Supplemental information for this paper.

4.1. Mineralogy and CEC of ICB overburden rocks

Major lithologic units surrounding the Pittsburgh coal seam include an underlying "underclay" and overlying carbon-rich shale, calcareous siltstone and sandstone, and calcareous mudstone (Fig. 2). Although drill logs for the FAY-051022 core identified the uppermost unit as argillaceous limestone, our XRD mineralogy and an acid dissolution mass balance indicate that lithology is calcareous mudstone.

Calcite and dolomite content of the overburden generally increased upward, from shale (4 %) to silt/sandstone (10 %) to calcareous mudstone (~25 %); these units are likely the primary contributors of alkalinity to CMD, as insignificant amounts of carbonate minerals were found in the underclay and Pittsburgh Coal (Fig. 2). Shale and silty sandstone units contain 2.5 % -5.0 % siderite, and reddish siderite veins were observed in the silty sandstone core material. Excluding coal, all units had high clay mineral content (19–39 %), emphasizing the importance of exchange reactions in the minepool aquifers.

Dominant exchangeable cations in the composite rock samples are Ca and Na, with average concentrations for replicate samples ranging from 0.11 to 0.38 meq/100 g and 0.01–0.18 meq/100 g, respectively, followed by Mg (0.01–0.09 meq/100 g) and K (0.001–0.02 meq/100 g); Al was below detection limit for all units except the sandstone (0.0002 meq/100 g) (Fig. S4).

CEC of montmorillonite, illite, and kaolinite standards are consistent with values reported in the literature for smectite CEC (60–150 meq/100 g), illite CEC (10–40 meq/100 g), and kaolinite (3–15 meq/100 g) respectively (Gülcan et al., 2017). CEC of the underclay (14.2 meq/100 g) and calcareous mudstone (11.4 meq/100 g) falls in the range of illite and bentonite clay standards and likewise has the highest Ca, Mg, and Na exchangeable ion concentrations (Figs. 2 and S4). High percentages (12–19 %) of illite-smectite mixed layer clays were found in the underclay and calcareous mudstone. The shale and sandstone had intermediate CEC (8.6 and 6.4 meq/100 g, respectively) and Na, Ca, and Mg ion concentrations, and fell more closely to the kaolinite standard. Pittsburgh coal seam had low CEC and exchangeable ion concentrations.

The exchangeable cation concentrations for each of the five lithology composites decreased in the order Ca > Na > Mg > K (Fig. S4). Relatively high exchangeable Ca suggests active exchange has taken place,

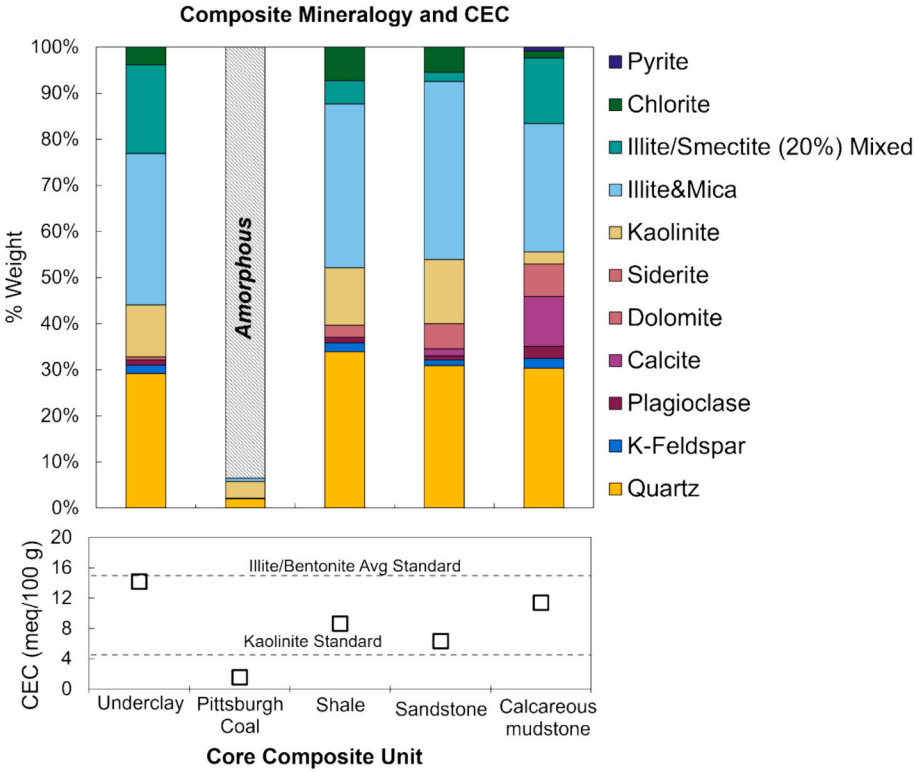

Fig. 2. Mineralogy determined by XRD (upper) and cation exchange capacity (CEC) (lower) for composite overburden lithologies from core FAY-051022. Clay standards shown for reference. The CEC is similar for illite (15.1 meq/100 g) and bentonite (14.9 meq/100 g) standards; that for montmorillonite (62.0 meq/100 g) is higher and not shown.

while abundant exchangeable Na plus relatively high CEC indicate potential for continued cation-exchange reactions, especially in the calcareous mudstone and underclay units. The original Na on the exchanger is expected to decrease as it is replaced by other cations from solution in the general selectivity order Ca > Mg > K > Na (Appelo, 1994; Appelo and Postma, 2005; Capuano and Jones, 2020).

4.2. Irwin Coal Basin spatial geochemical trends

The eight CMD sites exhibited increased pH, alkalinity, and Na concentrations from northeast to southwest across the ICB, coincident with increased Pittsburgh Coal seam mining depth. The two northernmost CMD sites, Export and Delmont, are net-acidic (median 89 and 32.5 mg/L as $CaCO_3$, respectively), whereas Irwin (median − 23 mg/L as $CaCO_3$) and Coal Run (median − 132 mg/L as $CaCO_3$) have intermediate net-acidity, and Lower and Upper Guffey, Lowber, and Douglas Run are highly mineralized with net-acidity median values less than −249 mg/L as $CaCO_3$.

4.2.1. Alkalinity production in the ICB

In this study, the DIC measured via CarboQC, used as the input component for inorganic C into PHREEQC, accurately speciates the CMD sites, and is important for understanding alkalinity production processes. Dissolved CO_2, expressed as $\log P_{CO2}$, ranged from −1.60 (Douglas Run) to −0.91 (Delmont) (Table S8), which are highly elevated in comparison to the atmospheric equilibrium value ($\log P_{CO2} = -3.4$). This is consistent with neutralization of sulfuric acid by carbonate minerals (Vesper et al., 2016). Calcite is highly undersaturated in the net-acidic discharges (median SI: −3.81 in Export and − 7.47 in Delmont) and remains undersaturated in net-alkaline discharges (−1.81 to −1.19) (Fig. S5).

The concentration of Na increases with alkalinity and depth, and median values range from 23 to 448 mg/L. The major-ion compositions of the ICB, illustrated in the Piper plot (Fig. 3), also reflect this trend, as the net-acidic sites are Ca-Mg-SO_4 type and the net-alkaline, deep mines are Na-SO_4-HCO_3 type. Acidic CMD that has been neutralized is typically Ca-Mg-SO_4 or Ca-Mg-SO_4-HCO_3 type water (McAuley and Kozar, 2006; Cravotta III and Brady, 2015), which contrasts with the observed chemistry of the alkaline CMD in the ICB. In the ICB, the molar ratios of Na and HCO_3 fall near the 2:1 M ratio line (Fig. S6A), which is indicative of calcite dissolution coupled with cation exchange ($CaCO_3 + H^+ +$

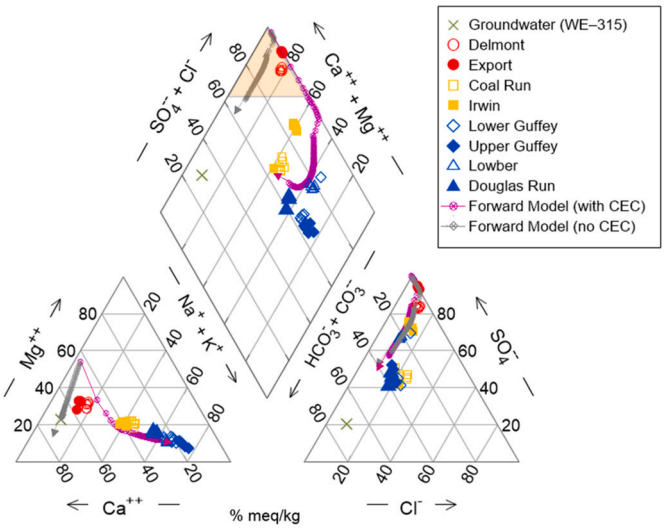

Fig. 3. Piper diagram of the major anions and cations of Irwin Coal Basin discharges (this study), and "background groundwater" (sample WE-315 of McAuley and Kozar, 2006). Typical AMD is shown in the shaded orange portion of upper graph. The evolutionary pathways of the forward reaction first flush model with and without cation exchange discussed in the text are also shown.

$Na_2EX = CaEX + 2Na^+ + HCO_3^-$). The coupled reactions can maintain calcite undersaturation (Fig. S5) and facilitate further calcite dissolution through the removal of Ca^{2+} from solution.

Additional data for northern Appalachian CMD ($n = 286$) show that the positive correlation between Na and alkalinity is a regional occurrence in deep minepools (Fig. S2). Molar Na and Cl values indicate that the excess Na observed in net-alkaline Appalachian CMD, including the ICB samples, does not originate from halite dissolution nor from deep brines found in the region (Fig. S2; Poth, 1962; Dresel and Rose, 2010). Therefore, the Na release (and Ca and Mg uptake) from exchange sites on overburden clay minerals during interaction with CMD is an important process associated with alkalinity production in this region (Cravotta III et al., 1994a; Perry, 2001; Bryant, 2002; Sharma et al., 2012). Cation exchange-driven alkalinity production is considered in the geochemical model presented in Section 4.5.

4.2.2. Fe attenuation in net-acidic to net-alkaline CMD

The high SO_4: Fe molar ratio (>2) from all sampled sites indicates that Fe is attenuated relative to SO_4 released by pyrite oxidation (Fig. S6B). Fig. 4 illustrates that Fe attenuation mechanisms differ along the net-acidic to net-alkaline geochemical transition across the basin. In the two net-acidic sites, Export and Delmont, Fe concentrations are controlled by the precipitation of Fe^{III} minerals such as jarosite, schwertmannite, and/or ferrihydrite, which are typical of above-drainage mines (e.g., Bigham et al., 1996; Burrows et al., 2015). Samples from both the Export and Delmont acidic CMD sites are slightly supersaturated with "schwertmannite(1.00)" having the composition $Fe_8O_8(OH)_{6.0}(SO_4)_{1.00}$ (logK 9.6, Majzlan et al., 2004), but are undersaturated with respect to schwertmannite having the composition $Fe_8O_8(OH)_{4.5}(SO_4)_{1.75}$ (logK 18, Bigham et al., 1996) and jarosite $(K_{0.77}Na_{0.03}H_{0.2})Fe_3(SO_4)_2(OH)_6$). All the CMD samples are supersaturated with goethite (FeOOH), but undersaturated with amorphous Fe $(OH)_3$ (Table S8), suggesting the potential for ferric hydroxide of intermediate solubility to maintain Fe^{III} concentrations. Although goethite is stable over the entire range of sampled pH, schwertmannite is more likely to precipitate from CMD at a pH of 2.8–4.5, whereas amorphous $Fe(OH)_3$ or ferrihydrite is favored at higher pH (Bigham et al., 1996; Nordstrom, 2011a, 2011b).

In contrast with the net-acidic, above-drainage CMD sites, the dissolved Fe in net-alkaline, below-drainage sources are elevated due to the predominance of Fe^{2+} in the samples and the relatively high solubility of ferrous oxyhydroxides and carbonates. Amorphous $Fe(OH)_3$ is slightly undersaturated, ranging from a median SI of −1.02 at Irwin to −0.16 at Douglas Run, whereas goethite is oversaturated. The siderite SI values for the net-alkaline CMD sites are near equilibrium (Coal Run median SI = −0.21; Lowber = 0.42), in contrast to the undersaturated conditions of the net-acidic CMD (median SI in Delmont is −2.04 and Export is −7.35) (Fig. S5b).

Siderite equilibrium is hypothesized to be an important, late-stage Fe attenuation mechanism that can maintain high Fe concentrations compared to Fe^{III} oxides. Therefore, Fe concentrations at equilibrium with siderite were considered in asymptote values for decay equations presented in Section 4.4 and geochemical models presented in Section 4.5.

4.3. Temporal variations and trends in pH, Fe, SO_4, and net-acidity

Since data were first reported in the 1970s, the pH of all ICB discharges has increased, and net-acidity, SO_4, and Fe concentrations have decreased (Fig. 5), consistent with trends reported for other long-term studies (e.g., Lambert et al., 2004; Burrows et al., 2015). However, the two above-drainage discharges, Delmont and Export, have maintained net acidic conditions for decades (Fig. 1). The decadal median pH for Export CMD has increased only slightly from 2.9 (1970s) to 3.2 (2020s), with consistently low Fe concentrations since the 1990s (0.8–3 mg/L). On the other hand, the pH in Delmont CMD increased from a median of

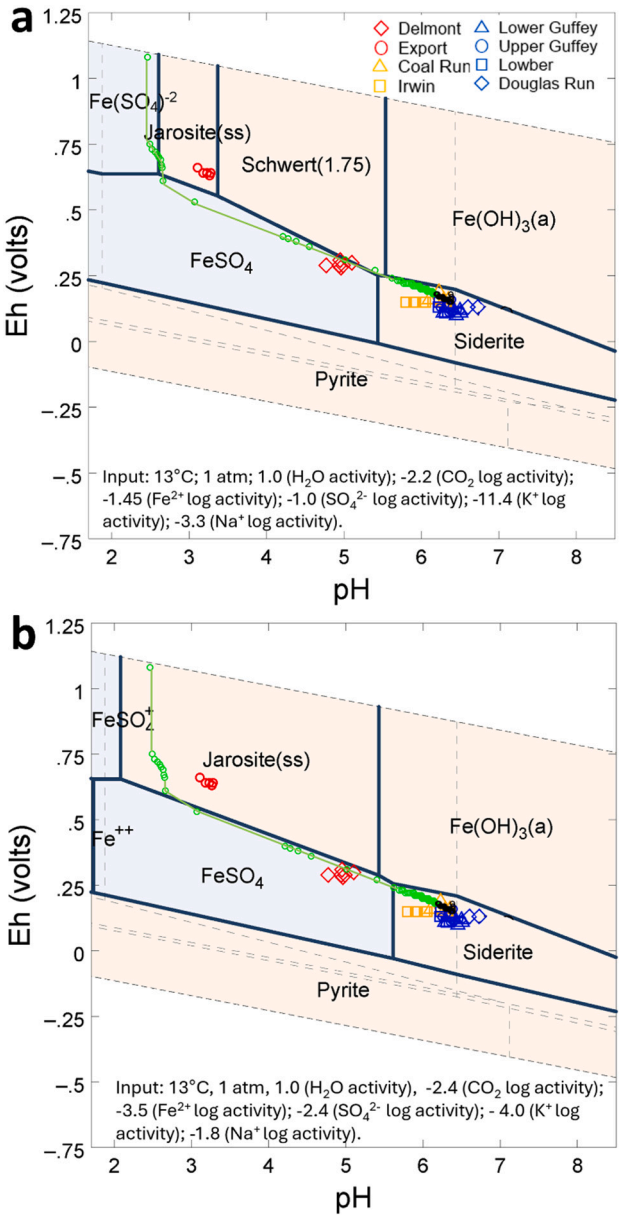

Fig. 4. Eh-pH diagram of the Irwin Coal basin sampling sites constructed with Geochemists Workbench Edition 17.0 (Bethke et al., 2021) and the wateq4f database using the median log activity values of Fe^{2+}, SO_4^{2-}, and pCO_2 calculated by PHREEQC for the first flush (a) and current conditions at Lowber (b). Measured values for ICB 2020–2021 samples are shown in legend. Progressive results at 1-year steps, from low to high pH, for first flush model involving mineral dissolution/precipitation plus CEC reactions are shown as smaller green (1953–2021) and black (2022–2053) symbols.

3.3 in the 1970s to ~5 since the 1990s, which indicates development of minor bicarbonate buffering, although the free-flow drainage may continue to be influenced by active pyrite oxidation. Iron in the Delmont discharge has remained essentially constant since the 1970s.

Lowber and Irwin CMD transitioned from net-acidic after 1973 to their current net-alkaline character. Although Fe and SO_4 concentrations have decreased for these below-drainage sites, they remain the highest in the ICB. This is likely due to continued water/mineral reactions along the CMD flowpath. Irwin CMD originates from a minepool influenced by adjacent shallow mines and groundwater (Winters and Capo, 2004). Since the 1970s, the Irwin CMD had the highest pH improvement (from a decadal median of 3.9 in the 1970s to 6.0 in the 2020s); pH in the Lowber discharge increased from a decadal median of 5.8 in the 1970s to

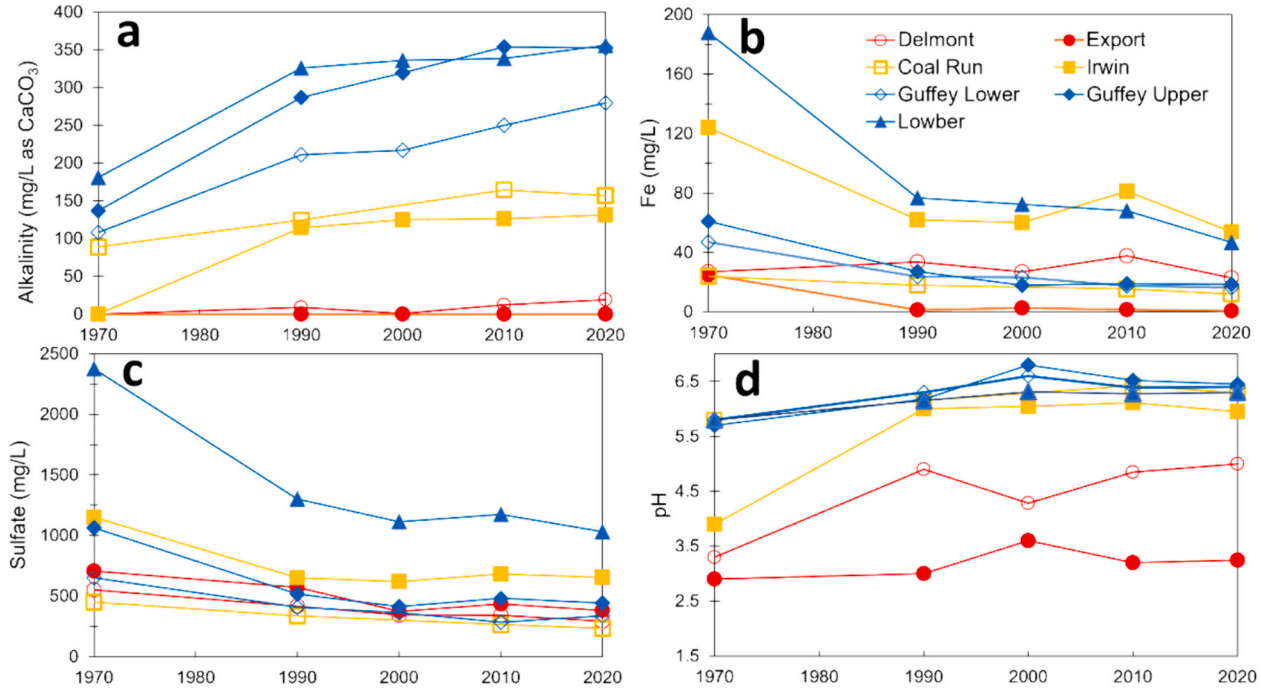

Fig. 5. Decadal median trends in ICB discharge chemistry. (a) Alkalinity; (b) dissolved iron; (c) sulfate; (d) pH. Data are not plotted for Douglas Run, which lacks historical data.

6.3 in the 2020s. In contrast, the Coal Run, Upper Guffey, and Lower Guffey discharges have remained net-alkaline within the available dataset, indicating that the net-acidic to net-alkaline transition occurred before 1973.

Although sampling data were not collected immediately after the mines closed across the basin (1910–1957), one approach to estimating the early-stage and future contaminant concentrations is to fit decay equations to historical data. All sites exhibited a drop in Fe, SO_4, and net-acidity concentrations since the 1970s (excluding the Fe trend in Delmont), followed by more gradual declines in the 1990s–2020s that reflect the first-flush contaminant decay. As a result, exponential decay models can be used to assess the evolution of CMD, as discussed in the following section.

4.4. First- and second-order decay models for Fe, SO_4, and net-acidity

First- and second-order rate equations (Eqs. (2)–(3)) were fit to long-term Fe, SO_4, and net-acidity data (annual medians for 1970's-2020's). Table S9 shows the nonlinear least squares regression results (C_0, k', k'' and the upper lower 95 % confidence bounds of the variables) and the specified steady-state contaminant levels (C_S values) for each of the seven CMD sites.

4.4.1. Steady-state contaminant considerations for major CMD contaminants

The decay equations used in this paper specify an asymptote value or steady-state term (C_S) to represent the eventual approach to background conditions. To calculate C_S values for each constituent, regional background groundwater conditions were evaluated (Table S10; McAuley and Kozar, 2006; Dempsey et al., 2002) along with realistic geochemical equilibrium constraints. Because of uncertainty in future conditions, Table S10 shows two C_S values calculated as an approximate range for each constituent. For SO_4, the specified C_S is based on local background conditions (35 mg/L; McAuley and Kozar, 2006) or a value of 50 mg/L, a minimum concentration introduced by Dempsey et al. (2002) that indicates CMD impacts to streams. The C_S terms calculated for the Fe models, 2.08 and 5.72 mg/L, assume the Fe concentration is maintained by equilibrium with crystalline or disordered siderite (logK values −10.89 or − 10.45, respectively), which is suggested by regional CMD data for samples with near-neutral pH (Cravotta III, 2008b). The C_S for net-acidity depends on the combination of pH, alkalinity, and metals concentrations per Eq. (4), considering equilibrium with siderite and calcite (Kirby and Cravotta III, 2005a, 2005b).

When selecting a steady-state value for any CMD site, site-specific geochemistry, such as pH, Fe stability fields, and the degree of flooding should be considered. For the ICB, the C_S values for Fe are notable because they are near or above the MCL for Fe in a permitted mine effluent in Pennsylvania (3 mg/L over a 30-day average; 7 mg/L maximum). Our first-order models project the Fe concentrations of the Lowber discharge 100 years after closure (2053) to be 16.8 mg/L (C_S = 2.08 mg/) or 18.4 mg/L (C_S of 5.72 mg/L). Concentrations of Fe and associated contaminants generally decrease through time; however, secondary minerals such as siderite may eventually become a source of Fe, rather than a sink, resulting in persistently elevated Fe concentrations that may warrant treatment. Using decay equations with values for the rate constant and steady-state asymptote constrained by geochemical processes can enhance future estimates of contaminants and also help to inform long-term remediation decisions.

4.4.2. Contaminant attenuation and depth of the minepool

Initial concentrations (C_0) and first-order rate constants (k') for the ICB sites increase with mine depth and flooding extent (Fig. S7A–D). We interpret this to result because the amount of pyrite available to oxidize and the amount of groundwater entering the system increases with overburden thickness. In northeastern USA, pyrite and leachable carbonates tend to be preserved at deeper levels of the bedrock as compared to shallow overburden, where such reactive minerals are depleted due to thousands of years of meteoric water exposure (Cravotta III et al., 1994b; Brady, 1998a). Additionally, groundwater with longer residence times has increased water-mineral reaction time, resulting in greater dissolution of carbonates and silicates and greater total dissolved solids (Brady, 1998b), which is consistent with the trend of higher C_0 with depth observed in the ICB. Groundwater influx is more extensive in deep mines, resulting in a greater dilution and rate of change in concentration

following the first flush, compared to shallower mines.

4.4.3. General confidence in fit of decay models

This study found that first-order decay models did not capture the initial rapid decline in contaminant concentrations, which could lead to incorrect forward projections. Second-order models may be a more accurate alternative that captures both the rapid decrease and long-term steady-state stages without increasing complexity (e.g., Zeman et al., 2009). However, the C_0 of second-order models could not be constrained due to a lack of early data. If early-stage data are available, second-order equations may be more applicable than first-order equations to describe CMD contaminant trends (i.e., Fig. S8). Further work on second-order decay models with specified steady-states on sites with early-time data is needed to confirm this. Limitations of first- and second-order decay equations are discussed in detail in Section 1.0 of Supplemental information.

4.5. First flush forward geochemical model

We applied the PHREEQC forward reaction model to indicate the relative importance of key processes that could account for observed first flush contaminant concentrations and corresponding trends in major solute concentrations and pH. Three model scenarios for the evolving minepool chemistry demonstrated effects of (1) dilution only without mineral dissolution or cation exchange; (2) dilution and mineral dissolution but without cation exchange; and (3) dilution, mineral dissolution, and cation exchange (Fig. 6).

Fig. 6 shows the forward model scenario incorporating cation-exchange reactions fits the observed data for the net-alkaline CMD better than the other scenarios. Simple mixing of groundwater with minepool water (green-dashed curves in Fig. 6c) results in the highest net acidity over the first ~60 years of minewater evolution. The most rapid drop in net acidity is observed in the models involving mineral dissolution plus cation exchange, due to enhanced alkalinity generation. Because of these differences, the timing for the net-acidity transition varies greatly among the models. Excluding cation exchange results in net-acidic CMD until year 53 in the flush cycle, whereas including cation exchange results in the net-alkaline transition between years 22–23, which more closely matches the observed data. Without cation exchange, cations in the ICB discharges remain dominated by Ca and Mg. (60–70 % Ca^{2+}; 30–40 % Mg^{2+}) (Fig. 3). However, with cation exchange, the discharge chemistry transitions from Ca-Mg-dominated water to Na-dominated water (70 %), which closely follows the observed geochemical trends for the ICB.

Additionally, cation exchange shifts the simulated trends for pH and Fe (Figs. 3 and 6). Interestingly, the modeled temporal changes in Eh and pH for Lowber are consistent with measured Eh and pH data plotted relative to Fe stability fields (Fig. 5). The simulated first-flush composition has very low pH and high concentrations of SO_4, Fe, and other dissolved metals plus high dissolved O_2 of ~13 mg/L, with corresponding Eh and pH values plotting at the boundary for atmospheric equilibrium (Fig. 5). The model demonstrates that as coquimbite and/or pyrite are dissolved by groundwater, very high concentrations of Fe are released into solution; however, under those conditions, various Fe^{III} or Fe^{II} minerals could feasibly precipitate, attenuating some of the Fe (Fig. 5). For example, in the scenario considering dilution, mineral reactions, and cation exchange, jarosite precipitation is modeled to account for the attenuation of Fe during years 1–17 (Table S8). An interim spike in Fe concentration around the 16–17-year interval corresponds to the transition from equilibrium with jarosite to amorphous $Fe(OH)_3$ (Fig. 6). Thereafter, from 17 to 91 years, oversaturation of both amorphous $Fe(OH)_3$ (SI > 0) and disordered siderite (SI > 0.3) results in their precipitation, with siderite attenuating the most Fe, generally about an order of magnitude more than $Fe(OH)_3$. During years 98–100, siderite is "undersaturated" (SI < 0.3, specified here), and $Fe(OH)_3$ precipitation accounts for removal of Fe.

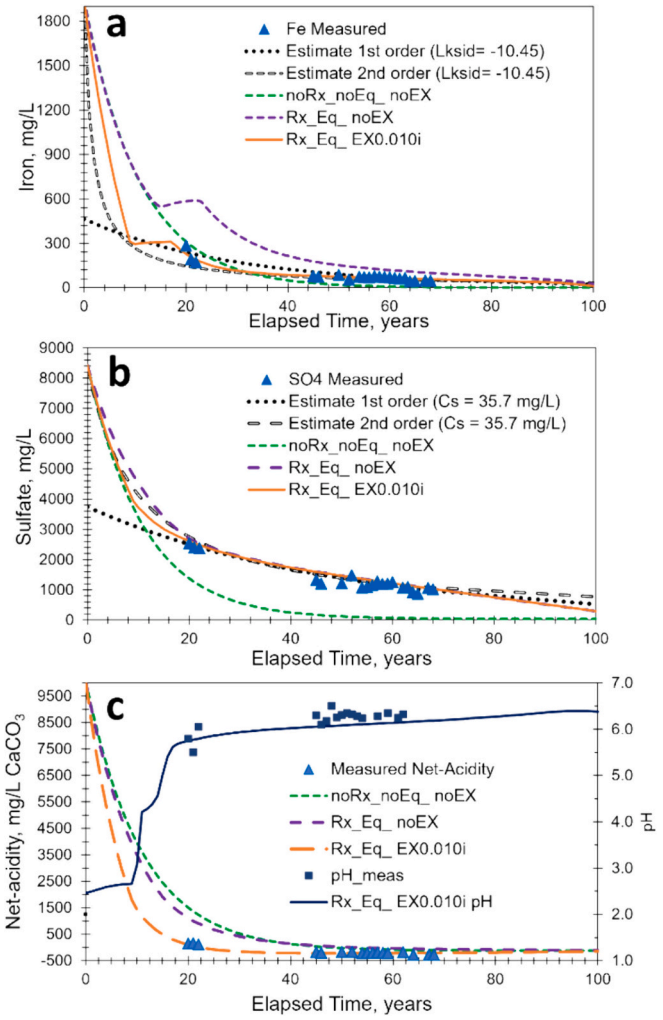

Fig. 6. First flush evolution model compared to observed water-quality data for the Lowber discharge. (a) Dissolved iron; (b) sulfate; (c) net acidity. The blue triangles and navy squares are measured values for the Lowber discharge; dotted and dashed black lines represent the first order and second order decay models, respectively, with specified steady-state value (C_S); dashed green curve (noRx_noeq_noEX) represents progressive mixing of minepool water and groundwater without additional reactions or cation exchange; dashed purple curve (Rx_Eq_noEX) represents progressive mixing and reactions, without cation exchange; orange or navy curves represent progressive mixing with reactions and cation-exchange (Rx_Eq_EX0.010i).

The novel aspect of this geochemical modeling approach is that physical and chemical processes are considered to explain observations of multiple interrelated constituents instead of using observed data points to determine decay functions for a given constituent, which may or may not be applicable to other constituents. Those processes are simulated to occur throughout time, considering realistic constraints such as the mixing ratio of groundwater (residence time), observed mineral reactants, eventual decay of the reactant phases, and anticipated equilibrium conditions for mineral precipitation/dissolution. Model results identify the dominant reactions that take place after pyrite is oxidized and initial CMD is produced by near-instantaneous dissolution of soluble oxidation products (SO_4 salts). After this initial flush of CMD, water in the minepool is progressively diluted and neutralized over time by inflows of alkaline groundwater coupled with the dissolution of carbonate minerals (with and without cation exchange), while progressively less pyrite oxidation takes place. Alkalinity is generated and cation exchange and mineral dissolution and precipitation occur as overburden minerals react with an evolving minepool fluid. The poor fit

of the observed SO_4 data compared to the simple dilution model indicates that there is continued active oxidation of pyrite in the subsurface (Fig. 6a, c), which is considered in the forward reaction model scenarios involving mineral dissolution. Likewise, the measured Fe concentrations from the Lowber discharge are approximately 1/5 of the value required to match FeS_2 stoichiometry, which indicates substantial Fe attenuation by mineral precipitation as modeled (Fig. 6a).

4.6. Conceptual model linking temporal and spatial evolution of minewater chemistry

A wide array of interactive physical and chemical processes accounts for the net-acidic to net-alkaline transition over time or along the CMD flowpath in the ICB. The first flush forward reaction model includes the influence of ambient groundwater chemistry that gradually replaces and mixes with the first flush CMD over time, combined with additional mineral dissolution and exchange reactions. This interaction is also reflected by depth-related chemical changes, with the shallower discharge sites representing earlier stages of a progressive geochemical evolution that transitions to the deeper minewater composition. In this context, the ICB can be considered a hydrosome, a hydrochemical groundwater system from a specific origin containing various geochemical facies that change along the flowpath, as described by Stuyfzand (1999).

The hydrosome shown in Fig. 7 represents a synthesis of results for this study and could be broadly applicable to Appalachian CMD chemistry; the ICB sites are shown for context. In general, minewater progresses from net-acidic to net-alkaline temporally and spatially, and the variations in major ion concentrations of the CMD sites are indicative of this transition. ICB sites in the hydrosome model are shown with increasing alkalinity, and generally depth, along the flowpath.

CMD evolution is constrained by spatiotemporal factors that can result in CMD geochemistry within the same basin being dominated by different water-rock interactions: acidity production, carbonate dissolution, cation-exchange, and siderite equilibrium. Mapping facies in a CMD hydrosome is a helpful way to share information on hydrogeochemical processes affecting remediation of abandoned or active mines.

5. Conclusions

The ICB system represents an excellent example of CMD spatial and temporal water-quality evolution and is a useful analog for understanding the evolution of water quality in abandoned mines or active mines that will eventually close and flood. The study documents net acidic to net alkaline CMD quality and changes in chemistry that culminate in the development of highly evolved Na-SO_4-HCO_3 type waters. Our data confirm that development of Na-rich water quality with elevated alkalinity results from the coupling of calcite dissolution and cation exchange with abundant clay minerals. High alkalinity and corresponding elevated P_{CO2} in deep minepools explain observed saturation to supersaturation with respect to siderite, which could result because the rate of calcite dissolution and corresponding alkalinity generation is faster than siderite precipitation. We conclude that siderite equilibrium could be a major factor maintaining elevated Fe concentrations in CMD over extended time.

Initial concentrations (C_0) of Fe, SO_4, and net-acidity were greater for the deeper mines, consistent with greater total mass of pyrite in thicker overburden. Greater first- and second-order rate constants for decay of these chemical parameters in the deeper mines were consistent with more extensive dilution by groundwater compared to intermediate to shallow depth mines. Rate models were improved by a specified steady-state asymptote (C_S) that considered background groundwater quality and geochemical constraints such as equilibrium with siderite and calcite. However, a lack of data and high uncertainty for initial "first-flush" conditions for historic mines resulted in difficulty estimating the C_0 term in the rate models, which complicates the use of first-order or second-order decay equations for future projections.

The first-flush geochemical model developed here considers physical and chemical processes that occur throughout time to explain observations and estimate trends rather than fitting exponential functions to observed data. The PHREEQC forward modeling quantifies the interaction of hydrological and geochemical processes over decadal time scales and indicates the potential for extrapolation of future water-quality trends while considering realistic constraints on availability of mineral reactants and solubilities. The modeling demonstrates that continuous mixing with ambient groundwater combined with reactions involving sulfide, carbonate, and silicate mineral dissolution and cation exchange are necessary to explain the observed changes in pH, alkalinity, Fe, Ca, Mg, and Na concentrations. These combined processes affect the timing and potential for the transition from net-acidic to net-alkaline conditions.

The results also highlight the importance of siderite, which can serve as a sink for Fe during the early stages of development of net alkaline water quality and also as a potential source of Fe during the later stages. Modeling with PHREEQC suggested that siderite is stable in the ICB minepools with net alkaline discharges. Siderite equilibrium could explain the commonly observed, sustained dissolved Fe content (>16 mg/L) in circumneutral CMD in the Appalachian Coalfield many

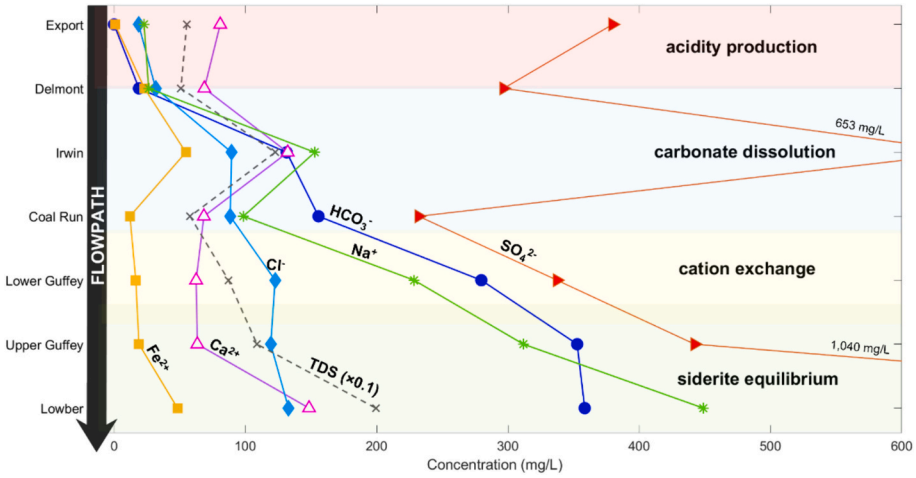

Fig. 7. Generalized geochemical facies of the Irwin Coal Basin along the net-acidic to net-alkaline flowpath through the minepools. Median concentrations for 2020–2021 for ICB CMD are plotted; sites are arranged in order of increasing net alkalinity. Total dissolved solids (TDS) are reported as 10 % median concentration and alkalinity (HCO_3^-) is reported in mg/L as $CaCO_3$.

decades after the first flush.

Accurate models of the long-term evolution of CMD chemistry are necessary to identify adaptive strategies for cost-effective remediation and to manage long-term post-mining obligations. Different technologies with varying costs may be applicable for future conditions, and eventually, no treatment may be necessary (Schaffer et al., 2024). These forward models bring us a step closer to being able to predict future pH and contaminant concentrations and could be applied to other mining sites with similar datasets. Ultimately, knowledge of the factors controlling net-acidic to net-alkaline transition and the evolution of associated contaminant concentrations in CMD can inform policy decisions about CMD remediation liability and treatment strategies.

Funding sources

Primary funding for this work was provided by a grant from the Office of Surface Mining Reclamation and Enforcement, Mine Drainage Technology Initiative (MDTI) program. Additional financial support was provided by the U.S. Geological Survey (USGS) for C. Cravotta while he worked on the study as a USGS employee; he is now retired from USGS. Any use of trade, firm, or product names is for descriptive purposes only and does not imply endorsement by the U.S. Government.

CRediT authorship contribution statement

C.R. Schaffer: Writing – original draft, Software, Investigation, Formal analysis. **C.A. Cravotta:** Writing – review & editing, Supervision, Software, Formal analysis, Conceptualization. **R.C. Capo:** Writing – review & editing, Supervision, Investigation. **B.C. Hedin:** Writing – review & editing, Investigation. **D.J. Vesper:** Writing – review & editing, Resources, Investigation. **B.W. Stewart:** Writing – review & editing, Investigation.

Declaration of competing interest

The authors declare that they have no known competing financial interests or personal relationships that could have appeared to influence the work reported in this paper.

Data availability

The data compiled for this study and the PHREEQC forward model are reported in Supplementary Information.

Acknowledgments

Helpful reviews of early drafts of this paper were provided by E. Perry and C. Jones (University of Pittsburgh). We thank the anonymous journal reviewers for detailed suggestions that greatly improved the manuscript. We thank W. Winters for sharing basin hydrology data and M. Wallace (West Virginia University) for carrying out CEC analyses.

Appendix A. Supplementary data

Supplementary data to this article can be found online at https://doi.org/10.1016/j.scitotenv.2024.174681.

References

Acharya, B.S., Kharel, G., 2020. Acid mine drainage from coal mining in the United States – an overview. J. Hydrol. 588, 125061 https://doi.org/10.1016/j.jhydrol.2020.125061.

Alpers, C.N., Nordstrom, D.K., 1999. Geochemical modeling of water-rock interactions in mining environments, In: Plumlee, G.S., . Logsdon, M.J. (eds.), The Environmental Geochemistry of Mineral Deposits. Part A. Processes, Methods, and Health Issues, Society of Economic Geologists, Littleton, Colorado, Reviews in Economic Geology 6A, chapter 14, p. 289–323. doi:https://doi.org/10.5382/Rev.06.

Alpers, C.N., Blowes, D.W., Nordstrom, D.K., Jambor, J.L., 1994. Secondary minerals and acid mine-water chemistry. In: Jambor, J.L., Blowes, D.W. (Eds.), Environmental Geochemistry of Sulfide Mine-wastes, Mineral. Assoc. Canada, Short Course Handbook, vol. 22, pp. 247–270.

American Public Health Association, 2000. 2320 alkalinity. In: Clesceri, L.S., Greenberg, A.E., Trussell, R.R. (Eds.), Standard Methods for the Examination of Water and Wastewater, 17th edition. American Public Health Association, Washington, pp. 35–39. http://hdl.handle.net/1969.3/24401.

Appelo, C.A.J., 1994. Cation and proton exchange, pH variations, and carbonate reactions in a freshening aquifer. Water Resour. Res. 30, 2793–2805. https://doi.org/10.1029/94WR01048.

Appelo, C.A.J., Postma, D., 2005. Geochemistry, Groundwater and Pollution (2nd). Balkema, Leiden, p. 678.

Ball, J.W., Nordstrom, D.K., 1991. User's manual for WATEQ4F with revised data base: U.S. Geological Survey Open-File Report 91-183, p.189. doi:https://doi.org/10.3133/ofr91183.

Bethke, C.M., Farrell, B., Yeakel, S., 2021. The Geochemist's Workbench Release 12 GWB Essentials Guide: Aqueous Solutions. LLC Champaign, Illinois. https://www.gwb.com/pdf/GWB12/GWBessentials.pdf.

Bigham, J.M., Schwertmann, U., Traina, S.J., Winland, R.L., Wolff, M., 1996. Schwertmannite and the chemical modeling of iron in acid sulfate waters. Geochim. Cosmochim. Acta 60 (12). https://doi.org/10.1016/0016-7037(96)00091-9.

Blowes, D.W., Ptacek, C.J., Jambor, J.L., Weisener, C.G., Paktunc, D., Gould, W.D., Johnson, D.B., 2014. The geochemistry of acid mine drainage. In: Sherwood Lollar, B. (Ed.), Environmental Geochemistry (2nd). Elsevier, pp. 131–190.

Brady, K.B.C., 1998a. Natural groundwater quality from unmined areas as a mine drainage quality prediction tool. In: Brady, K.B.C., Smith, M.W., Schueck, J.H. (Eds.), Coal Mine Drainage Prediction and Pollution Prevention in Pennsylvania. Pennsylvania Department of Environmental Protection, Harrisburg, pp. 8.1–8.92 (5600-BK-DEP2256).

Brady, K.B.C., 1998b. Groundwater chemistry from previously mined areas as a mine drainage quality prediction tool. In: Brady, K.B.C., Smith, M.W., Schueck, J. (Eds.), Coal Mine Drainage Prediction and Pollution Prevention in Pennsylvania. Pennsylvania Department of Environmental Protection, pp. 9.1–9.21.

Brady, K.B.C., Hornberger, R.J., Fleeger, G., 1998. Influence of geology on post-mining water quality-Northern Appalachian Basin. In: Brady, K.B.C., Smith, M.W., Schueck, J.H. (Eds.), Coal Mine Drainage Prediction and Pollution Prevention in Pennsylvania. Pennsylvania Department of Environmental Protection, Harrisburg, pp. 8.1–8.92 (5600-BK-DEP2256).

Bryant, E.M., 2002. Geochemical Modeling of Coal Mine Drainage from a Bituminous Coal Field in Western Pennsylvania. University of Pittsburgh, p. 96 (M.S. Thesis).

Burrows, J.E., Peters, S.C., Cravotta III, C.A., 2015. Temporal geochemical variations in above- and below-drainage coal mine discharge. Appl. Geochem. 62, 84–95. https://doi.org/10.1016/j.apgeochem.2015.02.010.

Capo, R.C., Winters, W.R., Weaver, T.J., Stafford, S.L., Hedin, R.S., Stewart, B.W., 2001. Hydrogeologic and geochemical evolution of deep mine discharges, Irwin syncline, Pennsylvania. Proc. 22nd W. Virginia Surface Mine Drainage Task Force Symposium, 144–153. https://wvmdtaskforce.com/wp-content/uploads/2016/01/01-capo.pdf.

Capuano, R.M., Jones, C.R., 2020. Cation exchange in groundwater-chemical evolution and prediction of paleo-groundwater flow: a natural-system study. Water Resour. Res. 56 (8) https://doi.org/10.1029/2019WR026318.

Chapman, E.C., Capo, R.C., Stewart, B.W., Hedin, R.S., Weaver, T.J., Edenborn, H.M., 2013. Strontium isotope quantifi- cation of siderite, brine and acid mine drainage contributions to high-TDS abandoned gas well discharges in the Appalachian Plateau. Appl. Geochem. 31, 109–118. https://doi.org/10.1016/j.apgeochem.2012.12.011.

Cravotta III, C.A., 1991. Geochemical evolution of acidic ground water at a reclaimed surface coal mine in western Pennsylvania. J. Am. Soc. Min. Reclam. 1, 43–68. https://doi.org/10.21000/jasmr91010043.

Cravotta III, C.A., 1994. Secondary iron-sulfate minerals as sources of sulfate and acidity: geochemical evolution of acidic ground water at a reclaimed surface coal mine in Pennsylvania. In: Alpers, C.N., Blowes, D.W. (Eds.), Environmental Geochemistry of Sulfide Oxidation, American Chemical Society Symposium Series, vol. 550, pp. 345–364. https://doi.org/10.1021/bk-1994-0550.ch023.

Cravotta III, C.A., 2008a. Dissolved metals and associated constituents in abandoned coal-mine discharges, Pennsylvania, USA. Part 1: constituent quantities and correlations. Appl. Geochem. 23, 166–202. https://doi.org/10.1016/j.apgeochem.2007.10.011.

Cravotta III, C.A., 2008b. Dissolved metals and associated constituents in abandoned coal-mine discharges, Pennsylvania, USA. Part 2: geochemical controls on constituent concentrations. Appl. Geochem. 23, 203–226. https://doi.org/10.1016/j.apgeochem.2007.10.003.

Cravotta III, C.A., 2008c. Laboratory and field evaluation of a flushable oxic limestone drain for treat- ment of net-acidic drainage from a flooded anthracite mine, Pennsylvania. USA. Appl. Geochem. 23, 3404–3422. https://doi.org/10.1016/j.apgeochem.2008.07.015.

Cravotta III, C.A., Brady, K.B.C., 2015. Priority pollutants and associated constituents in untreated and treated discharges from coal mining or processing facilities in Pennsylvania. USA. Appl. Geochem. 62, 108–130. https://doi.org/10.1016/j.apgeochem.2015.03.001.

Cravotta III, C.A., Dugas, D.L., Brady, K.B.C., Kovalchuk, T.E., 1994a. Effects of selective handling of pyritic, acid-forming materials on the chemistry of pore gas and ground water at a reclaimed surface coal mine in Clarion County, PA, USA. U.S. In: Bureau of Mines Special Publication SP 06A, pp. 365–374. https://doi.org/10.21000/JASMR94010365.

Cravotta III, C.A., Brady, K.B.C., Gustafson-Minnich, L.C., DiMatteo, M.R., 1994b. Geochemical and geohydrological characteristics of bedrock and mine spoil from two methods of mining at a reclaimed surface coal mine in Clarion County, PA, USA. In: U.S. Bureau of Mines Special Publication SP 06B, pp. 242–249. https://doi.org/10.21000/JASMR94020242.

Cravotta III, C.A., Goode, D.J., Bartles, M.D., Risser, D.W., Galeone, D.G., 2014. Surface-water and groundwater interactions in an extensively mined watershed, upper Schuylkill River, Pennsylvania, USA. Hydrol. Process. 28, 3574–3601. https://doi.org/10.1002/hyp.9885.

Cravotta III, C.A., Means, B., Arthur, W., McKenzie, R., Parkhurst, D.L., 2015. AMDTreat 5.0+ with PHREEQC titration module to compute caustic chemical quantity, effluent quality, and sludge volume. Mine Water Environ. 34, 136–152. https://doi.org/10.1007/s10230-014-0292-6.

Demchak, J., Skousen, J., McDonald, L.M., 2004. Longevity of acid discharges from underground mines located above the regional water table. J. Environ. Qual. 33, 656–668. https://doi.org/10.2134/jeq2004.6560.

Dempsey, B.A., Paksuchon, B., Suhataikul, R., Dietz, J., 2002. Sampling strategies for TMDL of AMD-affected streams. In: Proceedings of the 2002 National Meeting of the American Society of Mining and Reclamation, Lexington KY, June 9-13, 2002, pp. 10–26. https://doi.org/10.21000/JASMR02010010.

Dresel, P.E., Rose, A.W., 2010. Chemistry and origin of oil and gas well brines in Western Pennsylvania. In: Pennsylvania Geological Survey Open-File Report OFOG 10-01.0. http://www.docs.dcnr.pa.gov/cs/groups/public/documents/document/dcnr_015850.zip (48 p.).

Edmunds, W.E., 1999. Bituminous coal. In: Schultz, C.H. (Ed.), The Geology of Pennsylvania, Pennsylvania Geological Survey, 4th Series, Special Publication 1, pp. 470–481.

Eriksson, K.A., Daniels, W.L., 2021. Environmental implications of regional geology and coal mining in the Appalachians. In: Zipper, C.E., Skousen, J. (Eds.), Appalachia's Coal-mined Landscapes. Springer Nature, Switzerland, pp. 27–53. https://doi.org/10.1007/978-3-030-57780-3_2.

Gülcan, M., Özcan, Y., Küçükuysal, C., 2017. An experimental study on the mineralogical characte- rization of the Saribeyli kaolin deposit (Çanakkale, NW Turkey). Mugla J. Sci. Technol. 3, 4–8. https://doi.org/10.22531/muglajsci.295333.

Gyzl, G., Banks, D., 2007. Verification of the "first flush" phenomenon in mine water from coal mines in the Upper Silesian Coal Basin. Poland. J. Contam. Hydrol. 92, 66–86. https://doi.org/10.1016/j.jconhyd.2006.12.001.

Hedin Environmental, 2013. Irwin Discharge AMD Treatment System. Final Report for the Turtle Creek Watershed Association.

Huisamen, A., Wolkersdorfer, C., 2016. Modelling the hydrogeochemical evolution of mine water in a decommissioned opencast coal mine. Int. J. Coal Geol. 164, 3–12. https://doi.org/10.1016/j.coal.2016.05.006.

Kirby, C.S., Cravotta III, C.A., 2005a. Net alkalinity and net acidity 1: theoretical considerations. Appl. Geochem. 20, 1920–1940. https://doi.org/10.1016/j.apgeochem.2005.07.002.

Kirby, C.S., Cravotta III, C.A., 2005b. Net alkalinity and net acidity 2: practical considerations. Appl. Geochem. 20, 1941–1964. https://doi.org/10.1016/j.apgeochem.2005.07.003.

Lambert, D.C., McDonough, K.M., Dzombak, D.A., 2004. Long-term changes in quality of discharge water from abandoned underground coal mines in Uniontown Syncline, Fayette County, PA. USA. Wat. Res. 38, 277–288. https://doi.org/10.1016/j.watres.2003.09.017.

Langmuir, D. (1997) Aqueous Environmental Geochemistry. Prentice-Hall, Inc., Englewood Cliffs, 601.

Mack, B., Skousen, J., 2008. Acidity decay curves of 40 above drainage mines in West Virginia. Proc. Am. Soc. Min. Reclam. 612–627. In: https://www.asrs.us/Publications/Conference-Proceedings/2008/0613-Mack.pdf.

Majzlan, J., Navrotsky, A., Schwertmann, U., 2004. Thermodynamics of iron oxides. Part III. Enthalpies of formation and stability of ferrihydrite (~$Fe(OH)_3$), schwertmannite (~$FeO(OH)_{3/4}(SO_4)_{1/8}$), and e-$Fe_2O_3$. Geochim. Cosmochim. Acta 68, 1049–1059. https://doi.org/10.1016/S0016-7037(03)00371-5.

Majzlan, J., Navrotsky, A., McCleskey, R.B., Alpers, C.N., 2006. Thermodynamic properties and crystal structure refinement of ferricopiapite, coquimbite, rhomboclase, and $Fe_2(SO_4)_3(H_2O)_5$. Eur. J. Mineral. 18, 175–186. https://doi.org/10.1127/0935-1221/2006/0018-0175.

MathWorks Inc, 2023. MATLAB Version: 9.1.4 (R2023a). https://www.mathworks.com.

McAuley, S.D., Kozar, M.D., 2006. Ground-water quality in unmined areas and near reclaimed surface coal mines in the northern and central Appalachian coal regions, Pennsylvania and West Virginia. In: U.S. Geol. Surv. Sci. Invest. Rep. 2006-5059. https://pubs.usgs.gov/sir/2006/5059/pdf/sir2006-5059.pdf.

McDonough, K.M., Lambert, D.C., Mugunthan, P., Dzombak, D.A., 2005a. Hydrologic and geochemical factors governing chemical evolution of discharges from an abandoned, flooded underground coal mine network. J. Environ. Eng. 131, 643–650. https://doi.org/10.1061/(ASCE)0733-9372(2005)131:4(643).

McDonough, K.M., Lambert, D.C., Mugunthan, P., Dzombak, D.A., 2005b. Processes governing flow and chemical characteristics of discharges from free-draining, underground coal mines. J. Environ. Eng. 131, 1361–1368. https://doi.org/10.1061/(ASCE)0733-9372(2005)131:10(1361).

Mentz, J.W., Warg, J.B., 1975. Up-dip versus down-dip mining: an evaluation. EPA-670/2-75-047, United States Environmental Protection Agency. https://nepis.epa.gov/Exe/ZyPDF.cgi/9101VUCN.PDF?Dockey=9101VUCN.PDF.

Merritt, P., Power, C., 2022. Assessing the long-term evolution of mine water quality in abandoned underground mine workings using first-flush based models. Sci. Total Environ. 846, 157390 https://doi.org/10.1016/j.scitotenv.2022.157390.

Morrison, J.L., Atkinson, S.D., Sheetz, B.E., 1990. Delineation of potential manganese sources in the coal overburdens of western Pennsylvania. In: Proceedings of the 1990 Mining and Reclamation Conference and Exhibition, Charleston, West Virginia, April 23-26, 1990, vol. 1. West Virginia University, Morgantown, W.Va., pp. 249–256. https://doi.org/10.21000/JASMR90010249

Nordstrom, D.K., 1977. Thermochemical redox equilibria of ZoBell's solution. Geochim. Cosmochim. Acta 41, 1835–1841. https://doi.org/10.1016/0016-7037(77)90215-0.

Nordstrom, D.K., 2011a. Mine waters: acidic to circumneutral. Elements 7, 393–398. https://doi.org/10.2113/gselements.7.6.393.

Nordstrom, D.K., 2011b. Hydrogeochemical processes governing the origin, transport and fate of major and trace elements from mine wastes and mineralized rock to surface waters. Appl. Geochem. 26, 1777–1791. https://doi.org/10.1016/j.apgeochem.2011.06.002.

Nordstrom, D.K., 2020. Geochemical modeling of iron and aluminum precipitation during mixing and neutralization of acid mine drainage. Minerals 10, 547. https://doi.org/10.3390/min10060547.

Nordstrom, D.K., Campbell, K.M., 2014. Modeling low-temperature geochemical processes. In: Holland, H.D., Turekian, K.K. (Eds.), Treatise on Geochemistry (2nd), vol. v. 7. Elsevier, Oxford, pp. 27–68. https://doi.org/10.1016/B978-0-08-095975-7.00502-7.

Northern and Central Appalachian Basin Coal Regions Assessment Team, 2001. 2000 resource assessment of selected coal beds and zones in the Northern and Central Appalachian Basin coal regions. In: U.S. Geological Survey Professional Paper 1625-C. https://doi.org/10.3133/pp1625C.

Parkhurst, D.L., Appelo, C.A.J., 2013. Description of input and examples for PHREEQC Version 3—a computer program for speciation, batch-reaction, one-dimensional transport, and inverse geochemical calculations. In: U.S. Geol. Surv. Techniques Methods 6-A43. https://pubs.usgs.gov/tm/06/a43/ (497 p.).

Pennsylvania Department of Environmental Protection. Unpublished laboratory reports for samples collected by Pennsylvania Department of Environmental Protection during 2002-2006. Available per request or. https://gis.dep.pa.gov/esaSearch/ (variously dated).

Perry, E.F., 2001. Modeling rock-water interactions in flooded underground coal mines, northern Appalachian Basin. Geochem: Explor. Environ. Anal. 1, 61–70. https://doi.org/10.1144/geochem.1.1.61.

Perry, E.F., Rauch, H., 2012. Estimating water quality trends in abandoned coal minepools. 9th Int. Conf. Acid Rock Drain. 1, 1507–1519.

Perry, E.F., Rauch, H., 2013. Estimating water quality trends in abandoned coal minepools. In: West Virginia Mine Drainage Task Force Meeting, March 26–27, 2013, Morgantown, WV. https://wvmdtaskforce.files.wordpress.com/2016/01/13-perry-paper.pdf.

Perry, E.F., Hawkins, J., Dunn, M., Evans, R., Felbinger, J.K., 2005. Water quality trends in a flooded 35 year old mine pool. In: 22nd Amer. Soc. Mining Reclamation Ann. Conf, pp. 904–920. https://doi.org/10.21000/JASMR05010904.

Plummer, L.N., Busenberg, E., 1982. The solubilities of calcite, aragonite and vaterite in CO_2-H_2O solutions between 0 and 90°C, and an evaluation of the aqueous model for the system $CaCO_3$-CO_2-H_2O. Geochim. Cosmochim. Acta 46, 1011–1040. https://doi.org/10.1016/0016-7037(82)90056-4.

Poth, C.W., 1962. The occurrence of brine in western Pennsylvania. In: Pennsylvania Geological Survey Bulletin M-47.

Pötter, L., Krebs, N., Horstmann, M., Tollrian, R., Weiss, L.C., 2021. Long-term effects of elevated pCO_2 levels on the expression of Chaoborus-induced defences in *Daphnia pulex*. Zoology 146, 125909. https://doi.org/10.1016/j.zool.2021.125909.

Pullman Swindell Inc, 1977. Irwin Syncline Basin Mine Drainage Abatement Project, Operation Scarlift. Project no. SL 103-5, Department of Environmental Resources, Commonwealth of Pennsylvania. http://www.amrclearinghouse.org/Sub/SCARLIFT Reports/IrwinSyncline/IrwinSyncline.htm.

Raymond, P.A., Oh, N.-H., 2009. Long term changes of chemical weathering products in rivers heavily impacted from acid mine drainage: insights on the impact of coal mining on regional and global carbon and sulfur budgets. Earth Planet. Sci. Lett. 284, 50–56. https://doi.org/10.1016/j.epsl.2009.04.006.

Rose, A.W., Cravotta III, C.A., 1998. Geochemistry of coal mine drainage. In: Brady, K.B.C., Smith, M.W., Schueck, J. (Eds.), Coal Mine Drainage Prediction and Pollution Prevention in Pennsylvania. Pennsylvania Department of Environmental Protection, pp. 1.1–1.22.

Ruppert, L.F., Tewalt, S.J., Tully, J., Pierce, J., Weller, A., Yarnell, J., 1997. Map showing areal extent of the Pittsburgh Coal bed and horizon and mined areas of the Pittsburgh Coal Bed in Pennsylvania, Ohio, West Virginia, and Maryland. In: U.S. Geol. Surv. Open-File Report 96-280. https://pubs.usgs.gov/of/1996/of96-280/.

Schaffer, C.R., Cravotta, C.A.III, Capo, R.C., Stewart, B.W., Hedin, B.C., Vesper, D.J., 2024. Coal mine drainage contaminant trend prediction in an Appalachian basin, USA. In: Kleinmann, B., Skousen, J., Wolkersdorfer, Ch. (Eds.), West Virginia Mine Drainage Task Force Symposium & 15th International Mine Water Association Congress, Morgantown, WV, USA, pp. 555–561. https://www.imwa.info/docs/imwa_2024/IMWA2024_Schaffer_555.pdf.

Sharma, S., Sack, A., Adams, J.P., Vesper, D.J., Capo, R.C., Hartsock, A., Edenborn, H.M., 2012. Isotopic evidence of enhanced carbonate dissolution at a coal mine drainage site in Allegheny County, Pennsylvania. USA. Appl. Geochem. 29, 32–42. https://doi.org/10.1016/j.apgeochem.2012.11.002.

Skousen, J., 2017. Review of passive systems for acid mine drainage treatment. Mine Water Environ. 36, 133–153. https://doi.org/10.1007/s10230-016-0417-1.

Skousen, J.G., Ziemkiewicz, P.F., McDonald, L.F., 2019. Acid mine drainage formation, control and treatment: approaches and strategies. The Extractive Industries and Society 6, 241–249. https://doi.org/10.1016/j.exis.2018.09.008.

Stuyfzand, P.J., 1999. Patterns in groundwater chemistry resulting from groundwater flow. Hydrogeol. J. 7, 15–27. https://doi.org/10.1007/s100400050177.

Sumner, M.E., Miller, W.P., 1996. Cation exchange capacity and exchange coefficients. In: Sparks, D.L., Page, A.L., Helmke, P.A., Loeppert, R.H., Soltanpour, P.N.,

Tabatabai, M.A., Johnston, C.T., Sumner, M.E. (Eds.), Methods of Soil Analysis. https://doi.org/10.2136/sssabookser5.3.c40.

Thomas, J.F.J., Lynch, J.J., 1960. Determination of carbonate alkalinity in natural waters. J. Am. Water Works Assoc. 52 (2), 259–268. https://doi.org/10.1002/j.1551-8833.1960.tb00473.x.

Vass, C.R., Noble, A., Ziemkiewicz, P.F., 2019. The occurrence and concentration of rare earth elements in acid mine drainage and treatment by-products: part 1—initial survey of the northern Appalachian Coal Basin. Mining Metallurgy Explor. 36, 903–916. https://doi.org/10.1007/s42461-019-0097-z.

Vesper, D.J., Edenborn, H.M., 2012. Determination of free CO_2 in emergent groundwaters using a commercial beverage carbonation meter. J. Hydrol. 438–439, 148–155. https://doi.org/10.1016/j.jhydrol.2012.03.015.

Vesper, D.J., Moore, J.E., Adams, J.P., 2016. Inorganic carbon dynamics and CO_2 flux associated with coal-mine drainage sites in Blythedale PA and Lambert WV, USA. Environ. Earth Sci. 75, 340. https://doi.org/10.1007/s12665-015-5191-z.

Wang, C., Liao, F., Wang, G., Qu, S., Mao, H., Bai, Y., 2023. Hydrogeochemical evolution induced by long-term mining activities in a multi-aquifer system in the mining area. Sci. Total Environ. 854, 158806 https://doi.org/10.1016/j.scitotenv.2022.158806.

Weaver, T.J., Capo, R.C., Hedin, R.S., 1998. Geochemistry of deep mine waters in southwestern Pennsylvania and their evolution from acidic (AMD) to alkaline Fe contaminated discharges. In: Geol. Soc. Am. Abstr. Prog. 30, Charleston, WV.

Winters, W.R., Capo, R.C., 2004. Groundwater flow parameterization of an Appalachian coal mine complex. Ground Water 42, 700–710. https://doi.org/10.1111/j.1745-6584.2004.tb02724.x.

Wolkersdorfer, C., 2008. Water Management at Abandoned Flooded Underground Mines: Fundamentals, Tracer Tests, Modelling, Water Treatment. Springer, Berlin (459 p.).

Wood, C.R., 1996. Water quality of large discharges from mines in the Anthracite Region of eastern Pennyslvania. In: U.S. Geological Survey Water-Resources Investigations Report 95-4243. https://doi.org/10.3133/wri954243 (68 p.).

Wood, S.C., Younger, P.L., Robins, N.S., 1999. Long-term changes in the quality of polluted minewater discharges from abandoned underground coal workings in Scotland. Quart. J. Eng. Geol. Hydrogeol. 32, 69–79. https://doi.org/10.1144/GSL.QJEG.1999.032.P1.05.

Younger, P.L., 2000. Predicting temporal changes in total iron concentrations in groundwaters flowing from abandoned deep mines: a first approximation. J. Contam. Hydrol. 44, 47–69. https://doi.org/10.1016/S0169-7722(00)00090-5.

Yuan, H., Bish, D.L., 2010. Newmod+, a new version of the Newmod Program for interpreting X-ray powder diffraction patterns from interstratified clay minerals. Clay Clay Miner. 58, 318–326. https://doi.org/10.1346/CCMN.2010.0580303.

Zeman, J., Cernik, M., Supikova, I., 2009. Dynamic model of long term geochemical evolution of mine water after mine closure and flooding. Water Institute of Southern Africa. Mine Water Division. Proceedings of 2009 International Mine Water Association Conference. p. 828–836. https://www.imwa.info/docs/imwa_2009/IMWA2009_Zeman.pdf.